NANO LETTERS

Letter

Effect of Ion Distribution on Conductivity of Block Copolymer Electrolytes

Enrique D. Gomez, Ashoutosh Panday, Edward H. Feng, Vincent Chen, Gregory M. Stone, Andrew M. Minor, Christian Kisielowski, Kenneth H. Downing, Oleg Borodin, Grant D. Smith, and Nitash P. Balsara

Nano Lett., **2009**, 9 (3), 1212-1216• DOI: 10.1021/nl900091n • Publication Date (Web): 04 February 2009

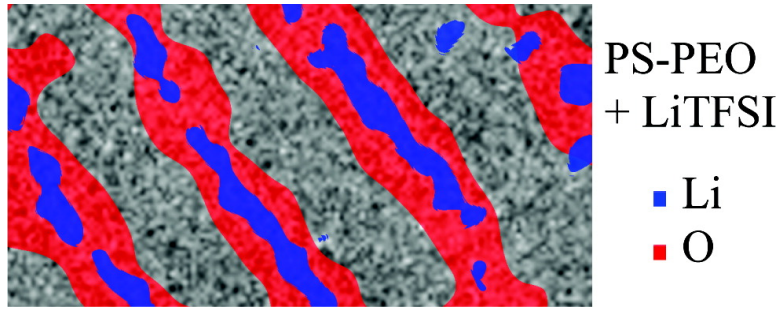

More About This Article

Additional resources and features associated with this article are available within the HTML version:

- Supporting Information
- Access to high resolution figures
- Links to articles and content related to this article
- Copyright permission to reproduce figures and/or text from this article

View the Full Text HTML

NANO LETTERS

2009
Vol. 9, No. 3
1212-1216

Effect of Ion Distribution on Conductivity of Block Copolymer Electrolytes

Enrique D. Gomez,[†,‡] Ashoutosh Panday,[†,§] Edward H. Feng,[†] Vincent Chen,[†] Gregory M. Stone,[†] Andrew M. Minor,[||,⊥] Christian Kisielowski,[||] Kenneth H. Downing,[#] Oleg Borodin,[▽] Grant D. Smith,[#] and Nitash P. Balsara*[,†,‡,§]

Department of Chemical Engineering, University of California, Berkeley, California 94720, Materials Sciences Division, Lawrence Berkeley National Laboratory, Berkeley, California 94720, Environmental Energy and Technologies Division, Lawrence Berkeley National Laboratory, Berkeley, California 94720, National Center for Electron Microscopy, Lawrence Berkeley National Laboratory, Berkeley, California 94720, Department of Materials Science and Engineering, University of California, Berkeley, California, 94720, Life Sciences Division, Lawrence Berkeley National Laboratory, Berkeley, California 94720, and Department of Materials Science & Engineering, 122 South Central Campus Drive, Room 304, University of Utah, Salt Lake City, Utah 84112-0560

Received January 11, 2009; Revised Manuscript Received January 27, 2009

ABSTRACT

Energy-filtered transmission electron microscopy (EFTEM) was used to determine the distribution of lithium ions in solid polymer electrolytes for lithium batteries. The electrolytes of interest are mixtures of bis(trifluoromethane)sulfonimide lithium salt and symmetric poly(styrene-*block*-ethylene oxide) copolymers (SEO). In contrast to current solid and liquid electrolytes, the conductivity of SEO/salt mixtures increases with increasing molecular weight of the copolymers. EFTEM results show that the salt is increasingly localized in the middle of the poly(ethylene oxide) (PEO) lamellae as the molecular weight of the copolymers is increased. Calculations of the inhomogeneous local stress field in block copolymer microdomains, modeled using self-consistent field theory, provide a quantitative explanation for this observation. These stresses, which increase with increasing molecular weight, interfere with the ability of PEO chains to coordinate with lithium cations near the walls of the PEO channels where ion mobility is expected to be low.

The distribution of ions in polymer matrices affects the properties and performance of a variety of devices.[1−6] Ion motion appears to be a limiting factor in device response time of polymer light-emitting diodes employing conjugated polyelectrolytes as electron transporting layers.[7] The distribution of ions in polymer electrolyte-gated organic transistors determines whether charge mobility is governed by electrostatic charging or electrochemical doping of the active layer.[8,9] Polymers that dissolve lithium ions are promising electrolyte materials for the next generation of rechargeable batteries.[10−14]

Applications such as rechargeable batteries require more from the electrolyte than high conductivity. High mechanical stability and high ionic conductivity can be achieved through microphase separated block copolymer electrolytes by using one phase to conduct ions while the other provides rigidity.[12−16] While the factors that underlie the conductivity of homogeneous polymer electrolytes are well established,[2,17−24] the effect of inhomogeneous morphology on ion transport is not well understood. Experimentally, it has been determined that the conductivity of block copolymer electrolytes increases with molecular weight and reaches a plateau when the copolymer molecular weight approaches 100 kg/mol.[14] This is in contrast to the trend in homopolymer electrolytes, where the conductivity decreases with increasing molecular weight and reaches a plateau when the homopolymer molecular weight approaches 1 kg/mol.[22]

[†] Department of Chemical Engineering, University of California, Berkeley.
[‡] Materials Sciences Division, Lawrence Berkeley National Laboratory.
[§] Environmental Energy and Technologies Division, Lawrence Berkeley National Laboratory.
[||] National Center for Electron Microscopy, Lawrence Berkeley National Laboratory.
[⊥] Department of Materials Science and Engineering, University of California.
[#] Life Sciences Division, Lawrence Berkeley National Laboratory.
[▽] Department of Materials Science & Engineering, University of Utah.

10.1021/nl900091n CCC: $40.75
Published on Web 02/04/2009

This qualitative difference between homopolymer and block copolymer electrolytes must reflect differences in the local environment of ions.

Energy-filtered transmission electron microscopy (EFTEM) has proven to be a convenient technique for determining the structure of ion-containing domains in polymer matrices. Previous efforts in this field are restricted to imaging ions with relatively large scattering cross sections such as cesium and cadmium.[25,26] In this paper we demonstrate that high-resolution EFTEM can be used to image the structure of lithium-containing domains in block copolymers. This is challenging due to the relatively small scattering cross section of lithium ions. While electron micrographs of crystalline structures with lithium atoms have been obtained in prior studies,[27,28] we are unaware of any previous reports on determining the structure of amorphous lithium-containing domains through the direct imaging of lithium in an electron microscope.

Our experiments were conducted on mixtures of poly(styrene-*block*-ethylene oxide) copolymers (SEO) and bis(trifluoromethane)sulfonimide lithium salt (LiTFSI). Blends were made in solution in an Ar glovebox and the polymer/LiTFSI mixtures were freeze-dried while preserving a moisture-free environment. Samples were hot-pressed at 120 °C into 0.1−0.2 mm films and annealed at 120 °C for 24 h prior to any experiment. The number of lithium ions per poly(ethylene oxide) monomer, r, was held fixed at 0.085 for all of the samples. Four SEO copolymers with varying molecular weights were synthesized by anionic polymerization as described in ref 14. The polymers are labeled SEO($x - y$) where x and y are the number-averaged molecular weights of the poly(styrene) (PS) and poly(ethylene oxide) (PEO) blocks in kg/mol, respectively. All copolymers have PEO volume fractions, f_{PEO}, close to 0.5 and exhibit lamellar morphologies. The characteristics of the polymers used in this study are tabulated in the Supporting Information. The chemical structures of SEO and LiTFSI are shown in Figure 1a. Previously, we obtained the domain spacing, d, of the copolymers used in this study using small-angle X-ray scattering (SAXS). We found that d scales with $N^{0.68}$ (N is the polymerization index), indicating that the copolymers are in the strong segregation limit.[14] Thin sections (ca. 50 nm) for electron microscopy were prepared using a cryomicrotome operating at −100 °C. Care was taken to minimize exposure to atmospheric water (see Supporting Information). Typical EFTEM results obtained from a Zeiss LIBRA 200FE microscope operating at 200 kV with an in-column Omega energy filter and an 8 eV slit are shown in Figure 1b where lithium, fluorine, and oxygen elemental maps of SEO(74-98)/LiTFSI using the three-window method[29] of the same region of the sample are shown. The light regions in Figure 1b correspond to the presence of the specific element of interest (Li, F, or O).[29,30] The lithium and fluorine elemental maps are a measure of the salt concentration within the block copolymer, while the oxygen map is a measure of the entire PEO domains. The salt anion also contains oxygen, but at $r = 0.085$ there are about three oxygen atoms in the polymer to every oxygen atom in the salt, and the oxygen map is

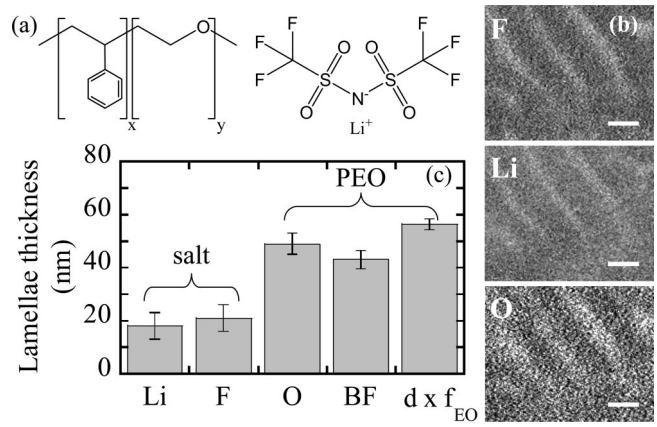

Figure 1. (a) Chemical structure of the SEO diblock copolymer and LiTFSI salt. (b) Elemental maps of F, Li, and O for SEO(74-98), $r = 0.085$. The scale bars are 50 nm. (c) Lamellae thickness using various measurement techniques for SEO(74-98)/LiTFSI. The first three columns correspond to measurements taken from EFTEM elemental maps ($r = 0.085$). The fourth column corresponds to the thickness of the PEO lamellae obtained from BF images obtained with RuO_4 staining ($r = 0$). The error bars are the standard deviation obtained from measurements over various regions. The last column is determined from SAXS data ($r = 0.085$). The first two columns correspond to the thickness of the Li lamellae, and the last three columns to the PEO lamellae width. It is clear that lithium is segregating to the middle of the PEO domains.

dominated by contributions from PEO. The similarity of the lamellar structures seen in Figure 1b indicates that the salt is sequestered within the PEO domains, as expected due to the well-established solubility of lithium salts in PEO and the nonpolar nature of PS. We note, however, that the absence of Li in our elemental maps means that the concentration of Li is below our detection limit and not necessarily zero. In the Supporting Information we quantify the Li detection limit of the Zeiss LIBRA microscope by comparing samples with different salt concentrations, and we estimate the limit to be $r = 0.04$. Results of quantitative analysis of several EFTEM images enables estimation of the thicknesses of Li, F, and O lamellae, and these results are given in Figure 1c. Accurate measurements of lamellae dimensions require considering the orientation of the lamellae with respect to the electron beam and the subjective nature of determining phase boundaries. A systematic approach was employed on all images, in a similar manner described previously to quantify the grain structures of block copolymers.[31,32] Details of this procedure are given in the Supporting Information. The thicknesses of the lamellae in the Li and F maps, 18 ± 5 and 21 ± 5 nm, respectively, are significantly smaller than that obtained from the O maps, 49 ± 4 nm for SEO(74-98)/LiTFSI with $r = 0.085$. Also included in Figure 1c is an estimate of the width of the PEO lamellae determined from bright-field TEM images of stained neat SEO(74-98) and from SAXS measurements. The thickness of the PEO lamellae obtained from these measurements is consistent with that obtained from the O EFTEM maps. It is clear from these results that the lithium salt is segregated to the middle of the PEO domains in SEO(74-98).

In Figure 2 we show typical EFTEM lithium elemental maps obtained from the SEO copolymers used in this study.

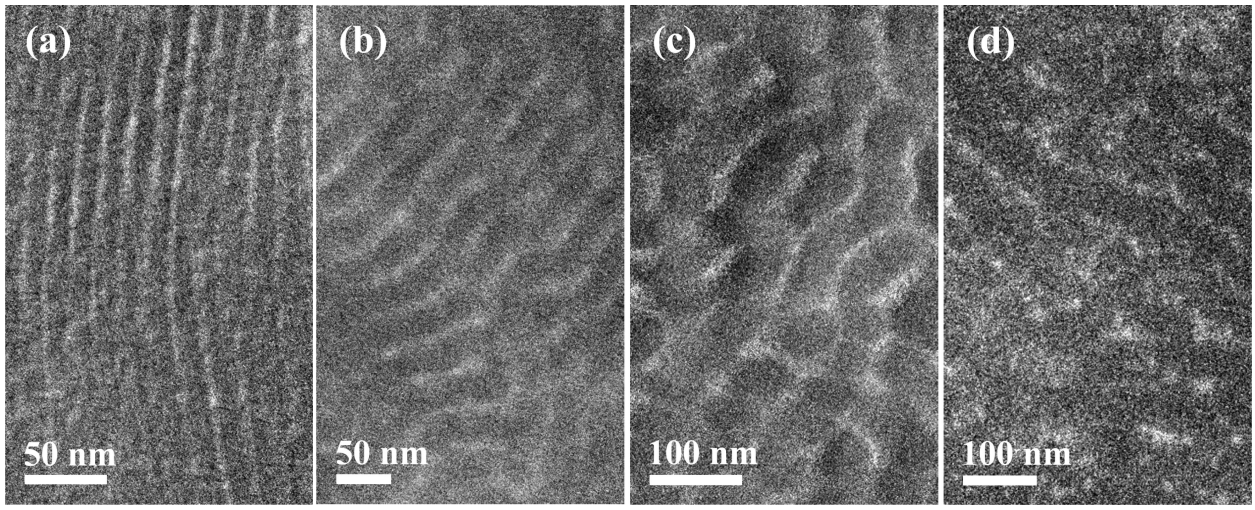

Figure 2. EFTEM Li maps of various unstained SEO copolymers ($r = 0.085$): (a) SEO(16-16); (b) SEO(40-31); (c) SEO(40-54); (d) SEO(74-98).

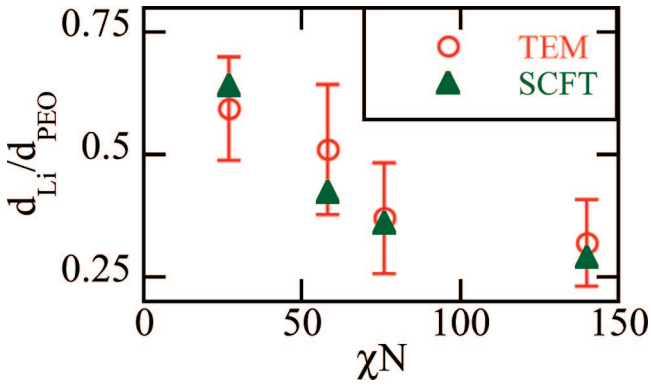

Figure 3. Relative Li lamellae thickness, d_{Li} (normalized by the width of the PEO lamellae, d_{PEO}), measured from experiments using TEM (open circles) and predicted from SCFT (solid triangles) versus χN. The error bars are the standard deviation obtained from measurements over various regions.

The long-range order of the copolymers appears to decrease with increasing molecular weight. Annealing, however, has no effect on the ionic conductivity of our copolymers (data not shown), suggesting that long-range order does not affect conductivity. This is supported by work on the diffusion of small molecules in block copolymers, where it was found that the diffusion coefficient does not depend on grain size.[33] Figure 2 enables an approximate determination of the lithium lamellae thickness, d_{Li}, of different samples. The width of the PEO domains, d_{PEO}, is obtained from the SAXS data, although $d_{PEO,SAXS}$ is quantitatively similar to $d_{PEO,TEM}$ (see Supporting Information). The ratio, d_{Li}/d_{PEO}, is plotted as a function of chain length in Figure 3 (open circles). We use the product χN as the abscissa in Figure 3 to facilitate comparisons with theoretical calculations. χ is the Flory−Huggins interaction parameter between PS and PEO chains at 80 °C,[34] and N is the number of repeat units per chain; both χ and N are based on a reference volume of 0.1 nm^3. It is clear from Figure 3 that the experimentally determined d_{Li}/d_{PEO} ratio decreases with increasing χN; i.e., the tendency for localization of Li^+ near the center of the PEO lamellae increases with increasing chain length.

We postulate that the nonuniformity of salt concentration within the PEO lamellae is related to the nonuniformity of Li^+/PEO coordination. The relationship between chain conformations and coordination of Li^+ ions with PEO homopolymer chains has been studied by molecular dynamics (MD) simulations.[35,36] This work shows that lithium is better coordinated by chains in nonextended conformations. Recent theoretical work based on self-consistent field theory (SCFT) has demonstrated methods for calculating the nonuniform chain stretching that occurs in ordered block copolymer phases.[37] Our analysis is based on both MD and SCFT results.

Previous MD simulation studies[36,38] of PEO/LiTFSI electrolytes have indicated that LiTFSI salt is almost completely dissociated by the PEO matrix for salt concentrations $r < 0.133$ with each Li^+ cation surrounded by four tightly bound and two loosely bound ether oxygens. For the case of SEO(74-98), the salt is localized to roughly one-third of the PEO lamella, indicating an upper limit for the local value of r of 0.175 ($1/r = 5.71$). Thus six ether oxygens are available for the preferred coordination between Li^+ and PEO despite localization of the salt.

The relationship between chain conformation and coordination between Li^+ and PEO can be obtained from MD simulations of lithium iodide dissolved in PEO chains with 12 repeat units presented in ref 35. In these simulations, it was shown that the radius of gyration (R_g) of the PEO chains decreases with increasing salt concentration due to coordination with Li^+. It is reasonable to propose that the inverse is also true; i.e., deformation of polymer chains also influences coordination between Li^+ and PEO. Using R_g determined from ref 35 at $T = 450$ K for $r = 0$, 0.02, and 0.067, $R_0^2/R^2 = 1.17$ at $r = 0.067$, where R is the radius of gyration of the perturbed chains (those coordinating cations) and R_0 is the radius of gyration of the same molecular weight PEO in the pure bulk melt. A linear extrapolation of R_0^2/R^2 from ref 35 to $r = 0.085$, the salt concentration in our system, gives $R_0^2/R^2 = 1.23$. The free energy penalty for changing the radius of gyration of a Gaussian chain from its unperturbed

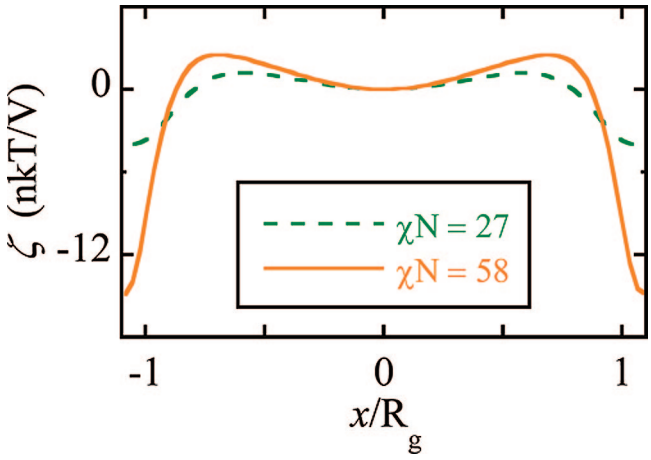

Figure 4. Local stress, ζ, proportional to the local chain stretching, as a function of position within the PEO domain of a copolymer with $\chi N = 27$, $f_{PEO} = 0.48$ (dashed line) and $\chi N = 58$, $f_{PEO} = 0.42$ (solid line), calculated using SCFT. The $\chi N = 27$ ($f_{PEO} = 0.48$) curve corresponds to SEO(16-16) and $\chi N = 58$ ($f_{PEO} = 0.42$) corresponds to SEO(40-31) at 80 °C.

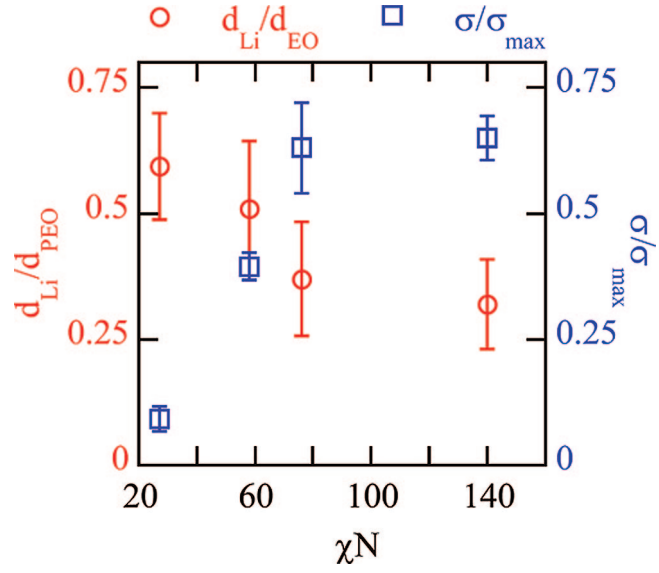

Figure 5. d_{Li}/d_{PEO} and normalized conductivity, σ/σ_{max}, as a function of molecular weight of the PEO chains, MW_{PEO}. The conductivity and Li segregation appear to be inversely correlated.

value R_0 to a value R in units of kT (k is the Boltzmann constant and T is absolute temperature) is given by $\zeta_d = (R^2/R_0^2 + R_0^2/R^2 - 2)$[39,40] which yields $\zeta_d = 0.043$ for our system.

SCFT is a coarse grained approach wherein each polymer chain is represented by a space curve $R(s)$ where s parametrizes the length of each polymer. The model captures the tendency for the end-to-end distribution of a polymer chain to be Gaussian, the chemical incompatibility of the A and B blocks quantified by the Flory−Huggins interaction parameter χ, and the incompressibility constraint. The local stress is characterized by $(dR(s)/ds)$.[2] Following ref 37, we calculated the deviatoric stress, ζ, or the actual stress minus the isotropic stress in the homogeneous phase. ζ is shown as a function of the position perpendicular to the lamellae, x, in units of R_g in Figure 4 for $\chi N = 27$ and 58 which corresponds to SEO(16-16) and SEO(40-31) at 80 °C, respectively.[34] Details concerning our SCFT calculations are given in the Supporting Information. One may interpret the numerical value of ζ as the local stretching energy per chain in units of kT. The stress in the x direction near the PS−PEO interface ($x \sim \pm 1.1$) is compressive with respect to the homogeneous phase due to the need to satisfy the constant density constraint at the interface between the A and B domains.[41] Moving away from the interface, the stress becomes positive, corresponding to chain stretching due to the chemical repulsion between the two blocks. At the middle of the domain, however, the chain stretching is zero.[37] While these general features are seen at all values of χN, the depth of the $\zeta(x)$ valley near the middle of the lamellae increases with increasing χN (Figure 4). It is important to note that the magnitudes of ζ are significantly larger than that of ζ_d, indicating that the deviatoric stresses in our block copolymers are larger than those needed to affect the coordination between lithium ions and PEO. Following the MD simulations, we propose that salt concentration is coupled to $\zeta(x)$. The large slope of the $\zeta(x)$ curve near the PS−PEO interface and the thermodynamic incompatibility of salt and PS (which is mixed into the PEO domains at the interface) leads to exclusion of the ions from this region. In the middle of the channels, we propose that if the local stress exceeds a certain critical value (in units of kT per chain), ζ^*, the PEO chains are unable to effectively coordinate with Li^+. This proposal enables calculation of an SCFT-based estimate of the value of d_{Li} by finding the region of the middle of the PEO lamellae where $\zeta < \zeta^*$. The filled symbols in Figure 3 show results of this calculation assuming that $\zeta^* = 1.6$. It is evident that the observation of increased confinement of Li ions in the middle of the PEO channels as molecular weight of the SEO copolymers increases is consistent with the SCFT predictions based on chain stretching. ζ_d, which is a factor of 40 lower than ζ^*, provides a lower bound on ζ^* as one expects the deformation energy required for complete loss of Li^+ coordination to be larger than ζ_d. Further work, such as the incorporation of the entropic penalty due to confinement of the salt, is needed to understand the underpinnings of the numerical factor relating ζ^* and ζ_d.

The normalized ionic conductivity, σ/σ_{max} (open squares), of SEO copolymers at 120 °C (well above the melting point of PEO) determined using ac impedance spectroscopy is plotted as a function of molecular weight of the PEO block in Figure 5. $\sigma_{max} = \phi_{PEO}\sigma_{PEO}$ where ϕ_{PEO} is the PEO volume fraction in the copolymer and σ_{PEO} is the measured conductivity of a 20 kg/mol PEO homopolymer at $r = 0.085$. This normalization allows us to compare our copolymer conductivities to the conductivity expected from PEO homopolymer. The molecular weight of the homopolymer is within the asymptotic region where the ionic conductivity does not change as a function of molecular weight.[22] The blend is amorphous in the 90−120 °C temperature range and σ/σ_{max} does not vary with temperature in this range (see Supporting Information). It is evident from Figure 5 that (σ/σ_{max}) approaches 2/3 at high molecular weights. This is the maximum conductivity expected from randomly oriented lamellae, since 1/3 of the diffusive steps are, on average,

ineffective.[14,42] The dependence of the normalized lithium lamellae thickness on molecular weight is also plotted in Figure 5. The inverse correlation between σ/σ_{max} and d_{Li}/d_{PEO} suggests that the distribution of the lithium ions within the PEO domains has an effect on the ionic conductivity. This can be attributed to slow lithium transport in systems with $d_{Li}/d_{PEO} \approx 1$ near the PS/PEO interface due to proximity to the glassy PS chains, the increased concentration of chain ends in the middle of the PEO channels, and, perhaps, differences in coordination due to local stresses.

In conclusion, we have measured the distribution of lithium salt in symmetric SEO block copolymers as a function of molecular weight using EFTEM. Arguments based on SCFT and MD simulations indicate that Li^+ cations are increasingly confined to the middle of the PEO lamellae due to nonuniform local stresses in the lamellae and the coupling between Li^+ coordination and these stresses. This effect leads to an unexpected increase in the ionic conductivity of block copolymer electrolytes with increasing molecular weight.

Acknowledgment. Major funding for this work was provided through the Electron Microscopy of Soft Matter Program at Lawrence Berkeley National Laboratory (LBNL) supported by the Director, Office of Science, Office of Basic Energy Sciences, Materials Sciences and Engineering Division, of the U.S. Department of Energy under Contract No. DE-AC02-05CH11231. The authors acknowledge support of the National Center for Electron Microscopy, Lawrence Berkeley Laboratory, which is supported by the U.S. Department of Energy under Contract # DE-AC02-05CH11231 PO No. 6515401. The Advanced Light Source is supported by the Director, Office of Science, Office of Basic Energy Sciences, of the U.S. Department of Energy under Contract No. DE-AC02-05CH11231.

Supporting Information Available: SCFT calculations, polymer synthesis, polymer and salt blending protocol, small-angle X-ray scattering results, ac impedance spectroscopy results, and energy-filtered transmission electron microscopy results. This material is available free of charge via the Internet at http://pubs.acs.org.

References

(1) Tarascon, J. M.; Armand, M. *Nature* **2001**, *414* (6861), 359–367.
(2) Meyer, W. H. *Adv. Mater.* **1998**, *10* (6), 439–448.
(3) White, H. S.; Kittlesen, G. P.; Wrighton, M. S. *J. Am. Chem. Soc.* **1984**, *106* (18), 5375–5377.
(4) Marsella, M. J.; Newland, R. J.; Carroll, P. J.; Swager, T. M. *J. Am. Chem. Soc.* **1995**, *117* (39), 9842–9848.
(5) Steele, B. C. H.; Heinzel, A. *Nature* **2001**, *414* (6861), 345–352.
(6) Kreuer, K. D.; Paddison, S. J.; Spohr, E.; Schuster, M. *Chem. Rev.* **2004**, *104* (10), 4637–4678.
(7) Hoven, C.; Yang, R.; Garcia, A.; Heeger, A. J.; Nguyen, T. Q.; Bazan, G. C. *J. Am. Chem. Soc.* **2007**, *129* (36), 10976–10977.
(8) Panzer, M. J.; Frisbie, C. D. *J. Am. Chem. Soc.* **2007**, *129* (20), 6599–6607.
(9) Lin, F. D.; Lonergan, M. C. *Appl. Phys. Lett.* **2006**, *88* (13), 133507.
(10) Gray, F. M.; Maccallum, J. R.; Vincent, C. A.; Giles, J. R. M. *Macromolecules* **1988**, *21* (2), 392–397.
(11) Cho, B. K.; Jain, A.; Gruner, S. M.; Wiesner, U. *Science* **2004**, *305* (5690), 1598–1601.
(12) Soo, P. P.; Huang, B. Y.; Jang, Y. I.; Chiang, Y. M.; Sadoway, D. R.; Mayes, A. M. *J. Electrochem. Soc.* **1999**, *146* (1), 32–37.
(13) Trapa, P. E.; Won, Y. Y.; Mui, S. C.; Olivetti, E. A.; Huang, B. Y.; Sadoway, D. R.; Mayes, A. M.; Dallek, S. *J. Electrochem. Soc.* **2005**, *152* (1), A1–A5.
(14) Singh, M.; Odusanya, O.; Wilmes, G. M.; Eitouni, H. B.; Gomez, E. D.; Patel, A. J.; Chen, V. L.; Park, M. J.; Fragouli, P.; Iatrou, H.; Hadjichristidis, N.; Cookson, D.; Balsara, N. P. *Macromolecules* **2007**, *40* (13), 4578–4585.
(15) Niitani, T.; Shimada, M.; Kawamura, K.; Dokko, K.; Rho, Y. H.; Kanamura, K. *Electrochem. Solid State Lett.* **2005**, *8* (8), A385–A388.
(16) Kishimoto, K.; Suzawa, T.; Yokota, T.; Mukai, T.; Ohno, H.; Kato, T. *J. Am. Chem. Soc.* **2005**, *127* (44), 15618–15623.
(17) MacCallum, J. R.; Vincent, C. A. *Polymer Electrolyte Reviews-1*; Elsevier Applied Science: London, 1987.
(18) Gray, F. M. *Polymer Electrolytes*; The Royal Society of Chemistry: Cambridge, 1997.
(19) Christie, A. M.; Lilley, S. J.; Staunton, E.; Andreev, Y. G.; Bruce, P. G. *Nature* **2005**, *433* (7021), 50–53.
(20) Gadjourova, Z.; Andreev, Y. G.; Tunstall, D. P.; Bruce, P. G. *Nature* **2001**, *412* (6846), 520–523.
(21) MacGlashan, G. S.; Andreev, Y. G.; Bruce, P. G. *Nature* **1999**, *398* (6730), 792–794.
(22) Shi, J.; Vincent, C. A. *Solid State Ionics* **1993**, *60* (1−3), 11–17.
(23) Chung, S. H.; Jeffrey, K. R.; Stevens, J. R. *J. Chem. Phys.* **1991**, *94* (3), 1803–1811.
(24) Fu, Y.; Pathmanathan, K.; Stevens, J. R. *J. Chem. Phys.* **1991**, *94* (9), 6323–6329.
(25) Moffitt, M.; Eisenberg, A. *Chem. Mater.* **1995**, *7* (6), 1178–1184.
(26) Kirkmeyer, B. P.; Taubert, A.; Kim, J. S.; Winey, K. I. *Macromolecules* **2002**, *35* (7), 2648–2653.
(27) O'Keefe, M. A.; Shao-Horn, Y. *Microsc. Microanal.* **2004**, *10* (1), 86–95.
(28) Shao-Horn, Y.; Croguennec, L.; Delmas, C.; Nelson, E. C.; O'Keefe, M. A. *Nat. Mater.* **2003**, *2* (7), 464–467.
(29) Egerton, R. F. *Electron energy-loss spectroscopy in the electron microscope*, 2nd ed.; Plenum Press: New York, 1996.
(30) Reimer, L. *Energy-Filtering Transmission Electron Microscopy*; Springer: Berlin, 1995.
(31) Chang, M. Y.; Abuzaina, F. M.; Kim, W. G.; Gupton, J. P.; Garetz, B. A.; Newstein, M. C.; Balsara, N. P.; Yang, L.; Gido, S. P.; Cohen, R. E.; Boontongkong, Y.; Bellare, A. *Macromolecules* **2002**, *35* (11), 4437–4447.
(32) Garetz, B. A.; Balsara, N. P.; Dai, H. J.; Wang, Z.; Newstein, M. C.; Majumdar, B. *Macromolecules* **1996**, *29* (13), 4675–4679.
(33) Kinning, D. J.; Thomas, E. L.; Ottino, J. M. *Macromolecules* **1987**, *20* (5), 1129–1133.
(34) Balsara, N. P.; Eitouni, H. B. Thermodynamics of Polymer Blends. In *Physical Properties of Polymer Handbook*, 2nd ed.; Mark, J. E., Ed.; Springer: New York, 2006.
(35) Borodin, O.; Smith, G. D. *Macromolecules* **1998**, *31* (23), 8396–8406.
(36) Borodin, O.; Smith, G. D. *Macromolecules* **2006**, *39* (4), 1620–1629.
(37) Maniadis, P.; Lookman, T.; Kober, E. M.; Rasmussen, K. O. *Phys. Rev. Lett.* **2007**, *99* (4), 048302.
(38) Borodin, O.; Smith, G. D. *J. Phys. Chem. B* **2006**, *110* (12), 6293–6299.
(39) Rubinstein, M.; Colby, R. H., *Polymer Physics*; Oxford University Press: New York, 2003.
(40) Leibler, L.; Orland, H.; Wheeler, J. C. *J. Chem. Phys.* **1983**, *79* (7), 3550–3557.
(41) Fredrickson, G. H. *The Equilibrium Theory of Inhomogeneous Polymers*; Oxford University Press: New York, 2006.
(42) Sax, J.; Ottino, J. M. *Polym. Eng. Sci.* **1983**, *23* (3), 165–176.

NL900091N